CALIBRATION AND EVALUATION OF ACCELEROMETERS BASED ON MULTISINUSOIDAL EXCITATION

Dariusz BUCHCZIK, Marek PAWEŁCZYK

Silesian University of Technology, Institute of Automatic Control, Measurement and Control Systems Group,
ul. Akademicka 16, 44-100 Gliwice, Poland,
e-mail: dariusz.buchczik@polsl.pl, marek.pawelczyk@polsl.pl

Abstract

Vibrational diagnostics of machines is usually based on use of accelerometers. Their calibration is required in order to obtain reliable results. This paper presents method for calibration of accelerometers using a multisinusoidal excitation. There is also proposed a procedure for estimating uncertainty of the obtained characteristics. The routine is based on an analysis of signals in the frequency domain using evaluation of cross power spectral density between the signals from the calibrated and standard accelerometer and evaluation of power spectral density of the signal from the standard accelerometer. The procedure allows to determine the nominal sensitivity, amplitude-frequency characteristics and estimate their uncertainties. The experiments were performed using a piezoelectric sensor PCB 338B35, and a sensor based on ADXL 202 capacitive accelerometer constructed at Silesian University of Technology. Results of this study show that the proposed method can be successfully used. The main advantage of the routine is a very short duration of the measurement experiment. Values of estimated relative uncertainties reach several percent. The procedure can be applied when it is necessary to quickly check the sensor characteristics, for example in the field for periodical maintenance of sensors mounted on the machine.

Keywords: accelerometers, calibration, uncertainty of measurements, vibration measurements

WYZNACZANIE CHARAKTERYSTYK AKCELEROMETRÓW Z WYKORZYSTANIEM POBUDZENIA WIELOSINUSOIDALNEGO

Streszczenie

Diagnostyka wibracyjna maszyn jest zwykle oparta na wykorzystaniu akcelerometrów. Ich kalibracja jest konieczna w celu uzyskania wiarygodnych wyników pomiarów. W artykule przedstawiono metodę wyznaczania charakterystyk akcelerometrów przy użyciu pobudzenia wielosinusoidalnego. Zaproponowano również procedurę szacowania niepewności uzyskanych parametrów. Metoda opiera się na analizie sygnałów w dziedzinie częstotliwości, przy wykorzystaniu oceny wzajemnej gęstości widmowej mocy pomiędzy sygnałami z czujników kalibrowanego i referencyjnego oraz oceny gęstości widmowej mocy sygnału z czujnika referencyjnego. Procedura umożliwia określenie czułości nominalnej, charakterystyki amplitudowo-częstotliwościowej oraz oszacowanie ich niepewności. Eksperymenty przeprowadzono stosując czujnik piezoelektryczny PCB 338B35 oraz czujnik oparty na akcelerometrze ADXL 202 skonstruowanym na Politechnice Śląskiej. Wyniki badań wskazują, że proponowaną metodę można z powodzeniem stosować. Główną zaletą procedury jest bardzo krótki czas trwania eksperymentu pomiarowego. Oszacowane względne niepewności osiągają kilkanaście procent. Procedura może być stosowana, gdy konieczne jest szybkie sprawdzenie charakterystyki czujnika, na przykład w warunkach polowych, przy okresowej konserwacji czujników zamontowanych na monitorowanej maszynie.

Słowa kluczowe: akcelerometry, kalibracja, niepewność wyników pomiarów, pomiary drgań

1. INTRODUCTION

Contemporary methods of calibration of accelerometers are based on the use of different concepts. Many proposals, especially for multi-axis accelerometers, utilize Earth's gravity acceleration [5], [8], [9] and advanced models of mathematical sensors [16], [19]. Although this approach allows for calibration in field conditions, the determination of dynamic characteristics of sensors is very limited. The use of auto-calibration feature also gives a less than satisfactory results due to the

nature of the excitation signal [6], [10]. Calibration in the low frequency range of several Hz requires the use of specific advanced vibration exciters [4], [11]. Laser interferometer technology provides the best results in a wide range of frequencies, but the cost of the equipment is very high [13], [14].

The method of calibration of accelerometers using uncommon excitation waveforms is not described in detail in the standards. In contrast to the method of comparison with the standard, which uses the effective values of the signals, the proposed method is based on an analysis of output

signals of a standard accelerometer and a calibrated accelerometer in the frequency domain [15]. Frequency characteristics of the accelerometers are determined using evaluation of cross power spectral density between the signals from the calibrated and standard accelerometer and evaluation of power spectral density of the signal from the standard accelerometer. Although, the calibration based on periodic, random and impulsive excitation is also presented in [12] and [1], the uncertainty estimation of calibration results exclusively for random excitation is proposed in [2].

2. PROCEDURE OF CALIBRATION

Latest ISO 16063-21 [7] standard describes the method of comparison with the standard but does not describe exactly procedure for calibration using waveforms other than sine wave. The possibility of a calibration based on random and multisinusiodal excitation is merely mentioned without a detailed description of this procedure.

According to the ISO 16063-21 standard suggested value of the relative expanded uncertainty of calibration shall not be larger than 2% in the frequency range from 0.4 Hz up to 1000 Hz, 4% for the range from 1 kHz up to 2 kHz or 6% in the range of 2 kHz to 10 kHz.

Representation of the time series in the frequency domain is the power spectral density. It contains information about the frequency structure of the signal. Moving from the time domain to the frequency domain is associated with Fourier transform.

The given continuous signal $x(t)$ is sampled with the period T_p:

$$x(i) = x(t)|_{t=iT_p}. \qquad (1)$$

The discrete time Fourier transform (1) is expressed by the equation:

$$X(j\Omega m) = T_p \sum_{i=0}^{N-1} [x(i)\exp(-j\Omega mi)]. \qquad (2)$$

Values of series (1) are known in the finite interval $i=0, 1, …, N−1$, and the frequency scale is divided into N segments, each with a length of one bin $\Omega = 2\pi/N$. In normalized frequency scale $F_p = 1/T_p$ corresponds to 2π.

The direct method of identification of power spectral density is based on the spectrum of the signal determined from the discrete Fourier transform. The power spectral density of the time-series (1) can be represented by the formula:

$$\hat{S}_{xx}^N = \frac{1}{NT_p} |X(j\Omega m)|^2, \qquad (3)$$

where: $m=0, 1, …, N−1$.

Measurement data may be disturbed by various factors. In this case, the smoothing operation can be used. The collected time sequence of length N samples is divided into L segments, each with a length of N_p samples. Evaluation of the power spectral density is performed for each segment.

Averaged power spectral density estimation is given by the formula:

$$\overline{\hat{S}_{xx}^N}(\Omega'm') = \frac{1}{L}\sum_{k=1}^{L}\hat{S}_{xx}^N(\Omega'm'), \qquad (4)$$

where: $m’=0, 1, … , N_p−1$; $\Omega’=2\pi/N_p$; $k=1, 2, …, L$.

If the input signal $u(i)$ and the output signal $y(i)$ from the system (sensor) are given, then by evaluating the power spectral density and the cross-power spectral density between the input and output signals, the evaluation of the amplitude-phase characteristic for the relative frequencies in the range $(0, \pi)$ can be estimated from the estimator:

$$\hat{G}^N(j\Omega m) = \frac{\hat{S}_{uy}^N(j\Omega m)}{\hat{S}_{uu}^N(j\Omega m)}. \qquad (5)$$

The cross-power spectral density estimate between the input $u(i)$ and output $y(i)$ signals is determined from:

$$\hat{S}_{uy}^N = \frac{1}{NT_p}U^N(-j\Omega m)Y^N(j\Omega m), \qquad (6)$$

and power spectral density estimate of output $y(i)$ signal:

$$\hat{S}_{uu}^N = \frac{1}{NT_p}|U(j\Omega m)|^2 = \frac{1}{NT_p}U^N(-j\Omega m)U^N(j\Omega m), \qquad (7)$$

where: $Y^N(j\Omega m)$ and $U^N(j\Omega m)$ are discrete Fourier transforms of the input $u(i)$ and output $y(i)$ signals determined from N samples according to (2).

Calibration based on comparison with the standard involves the use of the signals from the reference accelerometer (which is equivalent to the input signal $u(i)$) and the accelerometer under test (which is equivalent to the output signal $y(i)$). The signals are sampled and next split into L segments in order to perform an averaging operation in the course of further calculations. The amplitude-frequency characteristic and the phase-frequency characteristic for each of the L segments are calculated from formulas:

$$H_n(\Omega'm') = \left| \frac{\hat{S}_{uy}^{Np}(j\Omega'm')}{\hat{S}_{uu}^{Np}(j\Omega'm')} Q_r \right|, \qquad (8)$$

$$\varphi_n(\Omega'm') = \arg\left[\frac{\hat{S}_{uy}^{Np}(j\Omega'm')}{\hat{S}_{uu}^{Np}(j\Omega'm')} Q_r \right] + \varphi_r, \qquad (9)$$

where: $\hat{S}_{uy}^{Np}(j\Omega'm')$ is cross-power spectral density estimate between signals from reference and calibrated accelerometers, $\hat{S}_{uu}^{Np}(j\Omega'm')$ is power spectral density estimate of signals from reference accelerometer, Q_r is nominal sensitivity of reference accelerometer, φ_r is phase shift of reference accelerometer.

Eventually, there are determined the averaged amplitude-frequency and phase-frequency characteristic according to:

$$\overline{H(\Omega'm')} = \frac{1}{L}\sum_{n=1}^{L}H_n(j\Omega'm'), \qquad (11)$$

$$\overline{\varphi(\Omega'm')} = \frac{1}{L}\sum_{n=1}^{L}\varphi_n(j\Omega'm'). \qquad (12)$$

The multisinusoidal signal used for calibration is a sum of k sinusoidal signals that are periodic in time window of length N samples:

$$x(i) = \sum_{k=1}^{K} A_k \sin\left(\omega_k T_p i + \phi_k\right), \qquad (13)$$

where: $\omega_k T_p \in \left\{\dfrac{2\pi m}{N}; m = 1, 2, \ldots, \dfrac{N}{2}\right\}$.

An example of the multisinusoidal waveform signal and its power spectral density is shown in Fig. 1. The power spectral density estimate of the multisinusoidal signal is expressed by the relation:

$$S_{xx}^{N}(\omega m) = \begin{cases} \dfrac{T_p N}{4} A_k^2 & \text{for } \Omega m \in \left\{\omega_k T_p, 2\pi - \omega_k T_p\right\}, \\ 0 & \text{for } \Omega m \notin \left\{\omega_k T_p, 2\pi - \omega_k T_p\right\} \end{cases} \quad (14)$$

for m=0, 1,…, N-1.

2. ESTIMATION OF UNCERTAINTY

Estimation of the uncertainty type A is based on a statistical analysis of series of measurements. The best estimate of the expected (true) value of the measured quantity is the arithmetic mean of a series of measurements.

Estimation for the amplitude-frequency characteristic is possible due to the averaging of the characteristic on the basis of *L* values (number of segments). Uncertainty type A can be estimated only for particular relative frequency Ω'*m*' of the characteristic [2]. The true value of the characteristic is calculated according to (11) and (12).

Corrected sample standard deviation for the relative frequency Ω'*m*' equals:

$$\cdot \ \sigma_{H(\Omega'm')} = \sqrt{\dfrac{1}{L-1} \sum_{n=1}^{L} \left[H_n(\Omega'm') - \overline{H_n(\Omega'm')}\right]^2} \quad (15)$$
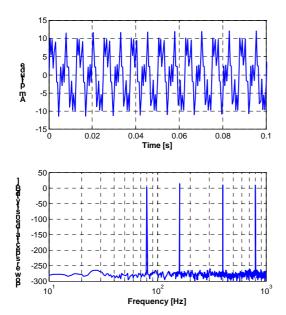

Fig. 1. Time waveform (left) and power spectral density (right) of exemplary multisinusoidal signal

Standard uncertainty type A for the relative frequency Ω'*m*' is computed as:

$$u_A = \sigma_{\overline{H(\Omega'm')}} = \dfrac{\sigma_{H(\Omega'm')}}{\sqrt{L}}. \qquad (16)$$

Consequently, relative standard uncertainty type A is given by:

$$u_A^o = \dfrac{\sigma_{\overline{H(\Omega'm')}}}{H(\Omega'm')}. \qquad (17)$$

The final result of the estimation is a set of uncertainties type A consisting of the uncertainties of averaged values, calculated according to (16) and (17), for all relative frequencies Ω'*m*'.

Estimation of the uncertainty type B refers to the calculation of uncertainty by means other than the statistical analysis of series of measurements. The standard uncertainty type B is determined by analysis based on all available information (accuracy specification of measurement instruments, results of previous calibration, etc.). Taking into account maximum permissible errors Δ_{gi} of all instruments on the test stand, the uncertainty type B of the test stand is calculated from the formula:

$$u_B = \dfrac{\sqrt{\sum_i \Delta_{gi}^2}}{\sqrt{3}}. \qquad (18)$$

Relative standard uncertainty type B equals:

$$u_B^o = \dfrac{\sqrt{\sum_i \delta_{gi}^2}}{\sqrt{3}}. \qquad (19)$$

Combined standard uncertainty taking into account the uncertainty of type A and B is determined from the equation:

$$u_C = \sqrt{u_A^2 + u_B^2}. \qquad (20)$$

Eventually, expanded uncertainty is the product of coverage factor k_α and the combined standard uncertainty:

$$U = k_\alpha u_C. \qquad (21)$$

The value of the coverage factor k_α is determined by the dominant uncertainty. For a small series of measurements, where the number segments *L*<10, the coverage factor is determined from the t-distribution for a confidence level of 95% and a degree of freedom $v = L$-1.

In the case of a larger number of segments *L*≥10 coverage factor is determined based on the normal distribution. Usually the confidence level of 95% is assumed, that results in k_α= 2.

2. TEST STAND

The test stand applied in the research is very similar to the typical measurement system dedicated to calibration of accelerometers using the method of comparison with the standard [7], [3]. The system is based on electromagnetic vibration exciter whose parameters limits frequency and amplitude range of the calibration. Instead of the

voltmeter which measures the effective voltage of output signals from the accelerometers a DAQ board is used, which allows measurement of the waveform at a certain sampling rate for further data processing in the frequency domain.

The equipment includes also a reference piezoelectric accelerometer type BK 8305S, a measuring amplifier type BK 2525 and a vibration exciter type BK 4809. The PXI platform from National Instruments equipped with a M-series DAQ board type PXI 6251 is used for waveform generation, measurement and data processing. The PXI system runs on Windows XP and Microsoft Office allows preparation of the reports. Access to the network facilitates the data transfer. A scheme of the system is shown in Fig. 2.

The total standard uncertainty type B of the test stand is u_B^o =4.2%. The dominant source of uncertainty type B is the error of multisinusoidal signal amplitude. Appropriate value of the amplitude is difficult to adjust due to nonlinearity of the vibration exciter and power amplifier.
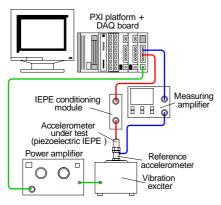

Fig. 2. Diagram of the measurement system
for calibration of accelerometers

The complex processing of the measurement data required to develop appropriate applications. Dedicated software written in LabView environment handle measurement and recording of measurement data, execute calculations and display resulting graphs, waveforms and parameters.

3. EXPERIMENTAL RESULTS

Studies on the calibration procedure were performed using two types of accelerometers. The first one is a single-axis IEPE piezoelectric sensor type PCB 338B35 and the second sensor, constructed in the Institute of Electronics of Silesian University of Technology, is based on a dual-axis capacitive accelerometer type ADXL 202.

The construction of the ADXL 202 based sensor is optimized for measurement of relatively small acceleration in the low frequency range. It is equipped with a simple low pass filter, which narrows the frequency band to 200 Hz. The amplitude-frequency characteristic of the sensor

determined using the method of comparison with the standard for acceleration of 10 m/s^2 is shown in Fig. 3.

The construction of sensors and their use for biomedical measurements are described in [3], [18] and for machine conditioning systems in [17].
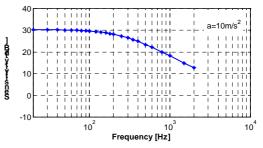

Fig. 3. Amplitude-frequency characteristic of
the sensor based on ADXL 202 capacitive
accelerometer determined using traditional
method for acceleration of 10 m/s^2

3.1. Calibration of piezoelectric accelerometer

The multisinusoidal signal, used during the calibration is composed of frequencies of 10, 12.5, 16, 20, 25, 31.5, 40, 50, 63, 80, 100, 125, 160, 200, 250, 315, 400, 500 , 630, 800, 1000, 1250, 1600, 2000, 2500 Hz (according to ISO 266) and accelerations of 3, 4, 5, 6, 7 m/s^2. The sampling frequency of acceleration signals was 6 kHz, the number of samples was 12000. The results have been determined for the following number of segments used to average characteristics: *L*=4, 8, 16, 32.

The resulting sensitivity characteristics of the piezoelectric accelerometer for various number of segments are shown in Fig. 4. The corresponding amplitude-frequency characteristics for the acceleration of 5 m/s^2 are presented in Fig. 5. The reference sensitivity of the accelerometer for 32 segments and reference frequency of 80 Hz is 9.21 mV/(m/s^2) (19.3 dB) with the expanded uncertainty of 0.42 mV/(m/s^2) whilst for 160 Hz the reference sensitivity is 9.73 mV/(m/s^2) (19.8 dB) with the expanded uncertainty of 0.43 mV/(m/s^2). Parameters of the piezoelectric accelerometer determined for various number of segments are summarized in Table 1.

Regardless of the number of segments, the parameters set differ very little, for a given reference frequency the differences do not exceed 1%. Increasing the number of segments practically does not affect the decrease of uncertainty. Type A uncertainty that can be reduced by increasing the number of segments (16) is small compared to the uncertainty of type B, which remains constant.

Sensitivity determined at 160 Hz is about 5% greater than the value for the 80Hz. The difference between the determined sensitivity for the 160 Hz and the sensitivity declared by the sensor manufacturer is relatively small and is about 5%.
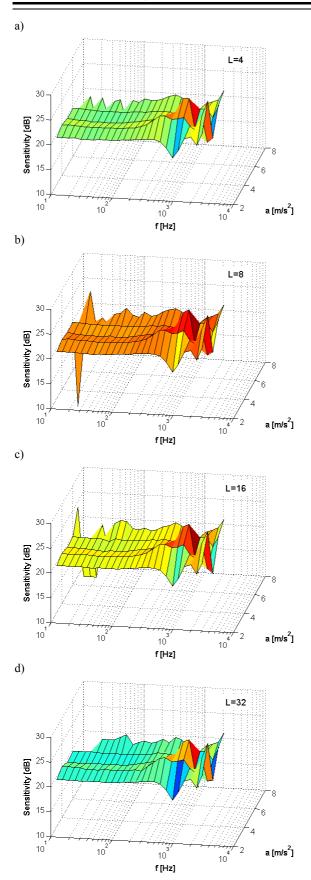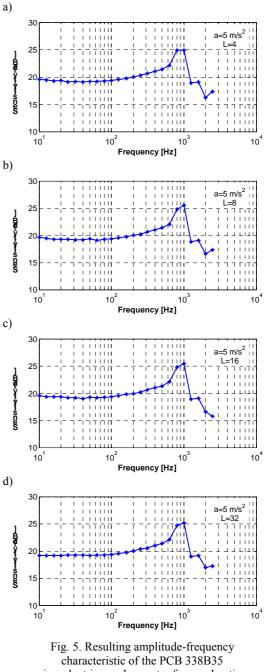
a)

b)

c)

d)

Fig. 4. Sensitivity characteristic of the PCB
338B35 piezoelectric accelerometer
determined for various number of segments:
a) *L*=4, b) *L*=8, c) *L*=16, d) *L*=32

a)

b)

c)

d)

Fig. 5. Resulting amplitude-frequency
characteristic of the PCB 338B35
piezoelectric accelerometer for acceleration
of 5 m/s² and various number of segments: a)
L=4, b) *L*=8, c) *L*=16, d) *L*=32

The same dependency can also be observed in
Fig. 5. The amplitude-frequency characteristic, is
flat to about 200 Hz, then the sensitivity increases.
The characteristic achieves a maximum at 1 kHz,
where the sensitivity is 80% greater than at the
reference frequency of 160Hz. The sensor
manufacturer declares deviation of 10% at
frequency of 3 kHz and a resonant frequency above
12 kHz. The corresponding uncertainty
characteristics, shown in Fig. 6, indicate an increase
in uncertainty only at a frequency greater than
800 Hz.

Table 1. Parameters of the piezoelectric accelerometer determined in course of experiments (for acceleration of 5m/s^2)

L	Sensitivity [mV/(m/s^2)]	Sensitivity [dB]	Relative uncertainty [%]	Uncertainty [mV/(m/s^2)]
	Reference frequency 80 Hz			
4	9.23	19.3	4.4	0.41
8	9.22	19.3	4.5	0.42
16	9.22	19.3	4.5	0.42
32	9.21	19.3	4.6	0.42
	Reference frequency 160 Hz			
4	9.76	19.8	4.4	0.43
8	9.75	19.8	4.4	0.43
16	9.80	19.8	4.7	0.46
32	9.73	19.8	4.5	0.43

The curve of the sensitivity characteristic shown in Fig. 4 becomes more irregular for acceleration over 6 m/s^2. There are visible large deviations from the nominal value, especially when number of segments is small (*L*=4, 8).

In conclusion, the best results are obtained for relatively small frequencies not exceeding 200 Hz and acceleration of less than 6 m/s^2. The reason for this phenomenon is the previously mentioned error of amplitude setting for a particular frequency component of the multisinusoidal signal.
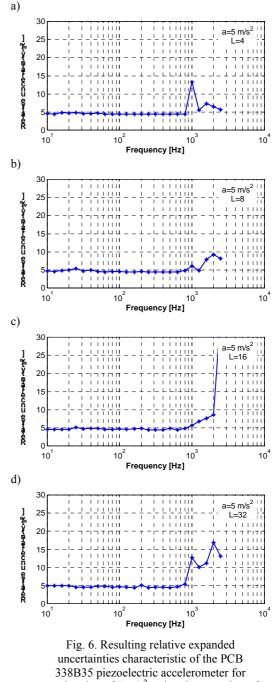
3.1. Calibration of capacitive accelerometer

The calibration of the capacitive accelerometer was accomplished using frequency component of 10, 12.5, 16, 20, 25, 31.5, 40, 50, 63, 80, 100, 125, 160, 200, 250, 315, 400, 500, 630, 800, 1000, 1250, 1600, 2000, 2500, 3150, 4000 Hz (according to ISO 266) and accelerations of 4, 5, 6, 7, 8 m/s2. Sampling frequency was 12 kHz, the number of samples was 24000 and number of segments was L=4, 8, 16, 32.

Basic parameters of the capacitive accelerometer obtained for various number of segments are presented in Table 2.

Table 2. Parameters of the capacitive accelerometer determined in course of experiments (for acceleration 7 m/s^2)

L	Sensitivity [mV/(m/s^2)]	Sensitivity [dB]	Relative uncertainty [%]	Uncertainty [mV/(m/s^2)]
	Reference frequency 80 Hz			
4	33.6	30.5	17	5.9
8	35.3	31.0	9.9	3.5
16	35.7	31.1	12	4.1
32	33.9	30.6	12	4.1
	Reference frequency 160 Hz			
4	25.8	28.2	8.5	2.2
8	27.3	28.7	11	2.9
16	29.6	29.4	18	5.4
32	29,1	29,3	19	5,7

a)

b)

c)

d)

Fig. 6. Resulting relative expanded uncertainties characteristic of the PCB 338B35 piezoelectric accelerometer for acceleration of 5 m/s^2 and various number of segments: a) *L*=4, b) *L*=8, c) *L*=16, d) *L*=32

The capacitive accelerometer has higher reference sensitivity with comparison to the piezoelectric one which is 33.9 mV/(m/s^2) for frequency of 80 Hz and 29.1 mV/(m/s^2) for frequency of 160 Hz. The corresponding expanded uncertainties are 4.1 mV/(m/s^2) and 5.7 mV/(m/s^2). The dispersion of parameters is much higher compared to the piezoelectric sensor. Depending on the number of segments, the sensitivity varies by about 4% for 80 Hz and about 10% for 160 Hz. The dispersion of uncertainties reaches over 100%, interestingly low uncertainties occur for small number of segments (L=4, 8).
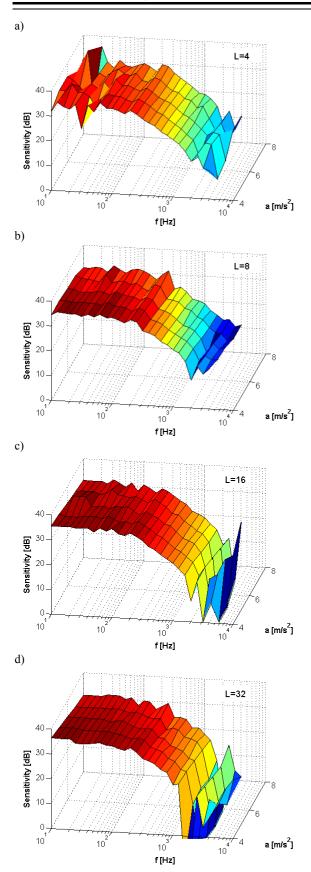
a)

b)

c)

d)

Fig. 7. Sensitivity characteristic of the sensor
based on ADXL 202 capacitive accelerometer
determined for various number of segments:
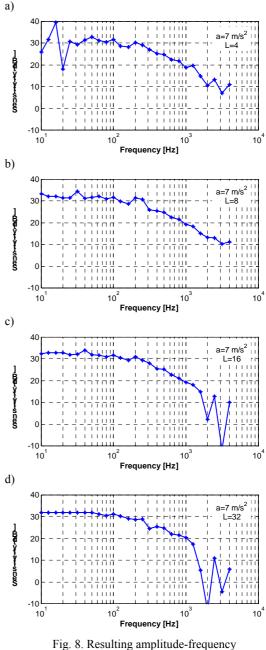a) *L*=4, b) *L*=8, c) *L*=16, d) *L*=32

a)

b)

c)

d)

Fig. 8. Resulting amplitude-frequency
characteristic of the sensor based on ADXL
202 capacitive accelerometer for acceleration
of 7 m/s² and various number of segments:
a) *L*=4, b) *L*=8, c) *L*=16, d) *L*=32

Analyzing the sensitivity characteristics
presented in Fig. 7, the amplitude-frequency
characteristics shown in Fig. 8 and uncertainty
characteristics displayed in Fig. 9, gives a better
picture of the situation and leads to different
conclusions.

The amplitude-frequency is very irregular for
small number of segments (*L*=4) and becomes more
flat with increasing number of segments (*L*=32).
The corresponding uncertainty characteristics for
L=4 show high values especially for a frequency
range up to 50 Hz. Next for the frequency up to
1 kHz the uncertainties are relatively low and
finally over 1 kHz their values increase again
rapidly. A similar pattern is also visible for *L*=8 and

16, but for *L*=32 uncertainties in low frequency range remain low.

a)

b)

c)

d)
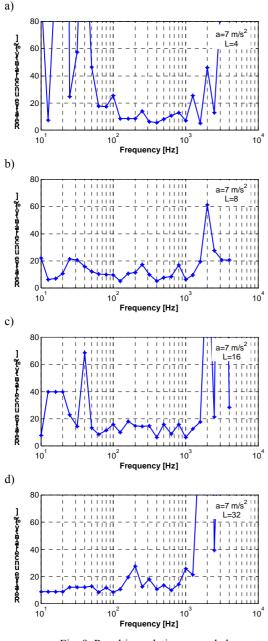

Fig. 9. Resulting relative expanded uncertainties characteristic of the sensor based on ADXL 202 capacitive accelerometer for acceleration of 7 m/s^2 and various number of segments: a) *L*=4, b) *L*=8, c) *L*=16, d) *L*=32

In summary, the increase in the number of segments provides a better shape of amplitude-frequency characteristics and lower uncertainties particularly for frequency up to 1kHz.

Analysis of the sensitivity characteristics shown in Fig. 7 leads to similar conclusions. For a large number of segments, the shape of the sensitivity plane is more regular and decrease in sensitivity due to low-pass filter operation is very well visible. Irregularities are visible only at frequencies above 1 kHz. The shape of the curve remains the same

regardless of the acceleration value. For small number of segments there are present irregularities at low frequencies and decrease in sensitivity caused by low-pass filtration is too slow.

Table 2. Parameters of the capacitive accelerometer determined in course of experiments (for acceleration of 7 m/s^2)

L	Sensitivity [mV/(m/s^2)]	Sensitivity [dB]	Relative uncertainty [%]	Uncertainty [mV/(m/s^2)]
Reference frequency 80 Hz				
4	33.6	30.5	17	5.9
8	35.3	31.0	9.9	3.5
16	35.7	31.1	12	4.1
32	33.9	30.6	12	4.1
Reference frequency 160 Hz				
4	25.8	28.2	8.5	2.2
8	27.3	28.7	11	2.9
16	29.6	29.4	18	5.4
32	29,1	29,3	19	5,7

6. CONCLUSIONS

Results of this study show that the method of calibration using multisinusoidal excitation can be successfully used to calibrate both piezoelectric and capacitive accelerometers, however, the uncertainty of the results is relatively large. The procedure allows to determine the nominal sensitivity for the reference frequency, amplitude-frequency and phase-frequency characteristics as well as estimation of the uncertainty of the results.

The best results are obtained for the frequency range up to 1 kHz using possibly a number of segments for averaging characteristics.

The most important advantage of the method based on multisinusoidal excitation with comparison to the classic method based on the sinusoidal excitation is very short duration of the measurement experiment. Usually it does not exceed a few seconds.

Values of uncertainty estimated during the calibration procedure for frequency reference are far larger than the ISO 16063-21 standard describes and they reach several percent. The method can be successfully applied when it is necessary to quickly check the accelerometer characteristics and large uncertainty of the results is acceptable, for example, in the field for the periodic maintenance of the sensors mounted on the object.

An important factor influencing the outcomes of the calibration are the number of sections used in averaging of the characteristics, the number of recorded samples and the sampling frequency. Further work on the optimal selection of these parameters can lead to a reduction in the uncertainty of the parameters and improving the designated characteristics.

LITERATURE

1. Albarbar A, Badri A, Sinha JK, Starr A. Performance evaluation of MEMS accelerometers. Measurement 2009; 42: 645-804. http://dx.doi.org/10.1016/j.measurement.2008.12.002
2. Buchczik D, Ryba A. Calibration of accelerometers using random excitation. Pomiary Automatyka Kontrola 2014; 8: 544-548.
3. Buchczik D, Wyżgolik R, Pietraszek S. Comparative study of acceleration transducers for biomedical applications, Proceedings of SPIE 2006, 6348: 63480U-1-63480U-10. http://dx.doi.org/10.1117/12.721118
4. D'Emilia G, Gaspari A, Natale E. (2015). Dynamic calibration uncertainty of three-axis low frequency accelerometers. ACTA IMEKO 2015; 4(4): 75-81. http://dx.doi.org/10.21014/acta_imeko.v4i4.239
5. Ferraris F, Grimaldi U, Parvis M. Procedure for effortless in-field calibration of three-axial rate gyro and accelerometers. Sensors and Materials 1995; 7.5: 311-330.
6. Frosio I, Pedersini F, Borghese NA. Autocalibration of MEMS accelerometers. IEEE Transactions on Instrumentation and Measurement 2009; 58(6): 2034-2041. http://dx.doi.org/10.1109/TIM.2008.2006137
7. ISO 16063-21 Methods for the calibration of vibration and shock transducers - Vibration calibration by comparison to a reference transducer. ISO 2003
8. Lötters JC, Schipper J, Veltink PH, Olthuis W, Bergveld P. Procedure for in-use calibration of triaxial accelerometers in medical applications. Sensors and Actuators A: Physical 1998; 68(1-3): 221-228. http://dx.doi.org/10.1016/S0924-4247(98)00049-1
9. Nez A, Fradet L, Laguillaumie P, Monnet T, Lacouture P. Comparison of calibration methods for accelerometers used in human motion analysis. Medical engineering & physics 2016; 38(11): 1289-1299. http://dx.doi.org/10.1016/j.medengphy.2016.08.004
10. Rocha LA, Dias RA, Cretu E, Mol L, Wolffenbuttel, RF. Auto-calibration of capacitive MEMS accelerometers based on pull-in voltage. Microsystem technologies 2011; 17(3): 429-436. http://dx.doi.org/10.1007/s00542-011-1252-8
11. Schiefer M, Bono R, Sill RD. Improved low frequency accelerometer calibration. In XIX Imeko World Congress-Fundamental and Applied Metrology.
12. Sinha JK. On standardisation of calibration procedure for accelerometer. Journal of Sound and Vibration 2005; 286: 417-427. http://dx.doi.org/10.1016/j.jsv.2004.12.004
13. Umeda A, Onoe M, Sakata K, Fukushia T, Kanari K, Iioka H, Kobayashi T. (2004). Calibration of three-axis accelerometers using a three-dimensional vibration generator and three laser interferometers. Sensors and Actuators A: Physical 2004; 114(1): 93-101. http://dx.doi.org/10.1016/j.sna.2004.03.011
14. von Martens HJ, Link A, Schlaak HJ, Taeubner A, Wabinski W, Goebel U. Recent advances in vibration and shock measurements and calibrations using laser interferometry. In Proceedings of SPIE 2004; 5503: 1-19. http://dx.doi.org/10.1117/12.579524
15. Wang FQ, Guo YZ, Xu XZ (1995) Influence of different excitation methods on vibration calibration. ISA Transactions 1995; 34: 87-92. http://dx.doi.org/10.1016/0019-0578(95)00002-H
16. Won, SHP, Golnaraghi F. A triaxial accelerometer calibration method using a mathematical model. IEEE Transactions on Instrumentation and Measurement 2010; 59.8: 2144-2153. http://dx.doi.org/10.1109/TIM.2009.2031849
17. Wyżgolik R, Buchczik D, Budzan S, Pawelczyk M. RT/FPGA implementation of the IEEE 1451 standard in sensors for machine conditioning systems. 21st International Conference on Methods and Models in Automation and Robotics (MMAR), Międzyzdroje, 2016,794-799. https://doi.org/10.1109/MMAR.2016.7575238
18. Wyżgolik R, Buchczik D, Pietraszek S. Low-frequency acceleration transducers for biomedical applications - the construction and the calibration. XXII Eurosensors, Dresden, 2008, Conference proceedings, 417-420.
19. Zhang L, Li W, Liu H. Accelerometer Static Calibration based on the PSO algorithm. In 2nd International Conference on Electronic & Mechanical Engineering and Information Technology. Atlantis Press 2012. http://dx.doi.org/10.2991/emeit.2012.119

Dariusz BUCHCZIK, Ph. D., assistant professor at the Institute of Automatic Control of the Silesian University of Technology in Gliwice. His research interests focus on robust estimation procedures using the least squares of median method, calibration and testing of acceleration sensors, vibrational diagnostics of machines.

Marek PAWEŁCZYK, Prof, DSc. He obtained his M.Sc. in 1995, Ph.D. in 1999, D.Sc. (habilitation) in 2005, and the scientific title of professor in 2014. He is currently a Full Titular Professor at the Silesian University of Technology. He is the Vice Rector (Vice President) for Science and Development of this university for the term 2016-2020. His main research interests focus on active noise-vibration control, digital signal processing, adaptive control and process identification.